Dissection of K^+ currents in *Caenorhabditis elegans* muscle cells by genetics and RNA interference

C. M. Santi*, A. Yuan*, G. Fawcett*, Z.-W. Wang*, A. Butler*, M. L. Nonet*, A. Wei*, P. Rojas*†‡, and L. Salkoff*§¶

Departments of *Anatomy and Neurobiology and §Genetics, Washington University School of Medicine, 660 South Euclid Avenue, St. Louis MO 63110; †Centro de Estudios Científicos, Valdivia 5119100, Chile; and ‡Facultad de Ciencias, Universidad de Chile, Santiago, Chile

GFP-promoter experiments have previously shown that at least nine genes encoding potassium channel subunits are expressed in *Caenorhabditis elegans* muscle. By using genetic, RNA interference, and physiological techniques we revealed the molecular identity of the major components of the outward K^+ currents in body wall muscle cells in culture. We found that under physiological conditions, outward current is dominated by the products of only two genes, *Shaker* (Kv1) and *Shal* (Kv4), both expressing voltage-dependent potassium channels. Other channels may be held in reserve to respond to particular circumstances. Because GFP-promoter experiments indicated that *slo-2* expression is prominent, we created a deletion mutant to identify the SLO-2 current *in vivo*. In both whole-cell and single-channel modes, *in vivo* SLO-2 channels were active only when intracellular Ca^{2+} and Cl^- were raised above normal physiological conditions, as occurs during hypoxia. Under such conditions, SLO-2 is the largest outward current, contributing up to 87% of the total current. Other channels are present in muscle, but our results suggest that they are unlikely to contribute a large outward component under physiological conditions. However, they, too, may contribute currents conditional on other factors. Hence, the picture that emerges is of a complex membrane with a small number of household conductances functioning under normal circumstances, but with additional conductances that are activated during unusual circumstances.

Because of its versatile genetic and molecular resources, and the recent development of both cell culture (1) and physiological techniques in *Caenorhabditis elegans* (2, 3) this model animal system offers unique advantages to dissect the contributions of the many ion currents in the membrane of a single cell type. Surprisingly, *C. elegans* was found to have an inventory of >70 potassium channels in its genome (4, 5), suggesting a high degree of complexity in its membrane electrical properties. Promoter-GFP experiments indicated that, in the muscle membrane alone, there are at least nine K^+ channel types present (3, 4, 6). These channels include voltage-dependent K^+ channels, high conductance channels activated by intracellular ions, and several "twk" channels. A prior study observed both transient and noninactivating outward currents in adult body wall muscle cells from *C. elegans* but their molecular identity was not established (7). In this study, we have used the combined resources of *C. elegans* to reveal the molecular-genetic basis for the channels that account for most of the outward current. The results suggest that under "typical" physiological conditions commonly used in electrophysiological studies, voltage-dependent outward potassium currents predominate. By using a combination of genetic and RNA interference (RNAi) techniques we revealed that the voltage-dependent component was composed of two currents, SHAL (Kv4) and SHAKER (Kv1). However, we also showed that the membrane contains "reserve" conductances, which may be even larger and conditional upon special circumstances. We found that a major reserve conductance is carried by SLO-2 channels, the *C. elegans* orthologue of the mammalian sodium-activated potassium channel (8). SLO-2 may be the most abundantly expressed potassium channel in *C. elegans*, as suggested by the higher representation of the *slo-2* gene in the *C. elegans* EST database compared with other K^+ channel genes (4). SLO-2 channels heterologously expressed are activated by high intracellular concentrations of chloride and calcium ions, intracellular conditions not seen under normal physiological circumstances, but conditions that could be achieved under hypoxia (9). *Slo-2* mutants were shown to be hypersensitive to hypoxia (8), suggesting a role for *slo-2* in protecting cells under hypoxic stress. In native cells we found that the SLO-2 current was almost five times larger than the voltage-dependent components under conditions of elevated intracellular chloride and calcium ions. This result was confirmed by mutant analysis that showed that this unusually large conductance was absent in *slo-2* mutants. Other conductances present in the muscle membrane may include twk "two-pore" channels, (4, 10). Such channels could contribute to resting membrane conductance or could be conditional on a variety of stimuli such as temperature or pH (11).

Although these results do not account for the activity of all potassium channels present in the membrane, the combined molecular and genetic techniques available in *C. elegans* are helping to reveal a more complete picture of the full palette and complexity of potassium channels present in a single membrane.

Materials and Methods

***slo-2* Mutants.** Using a modification of PCR-based screens for targeted gene deletions (12, 13), we isolated two *slo-2* deletion mutants as described (14). One of the deletion mutants [*slo-2 (nf 100)*] contains an in-frame deletion removing a highly conserved region in the cytoplasmic carboxyl region of *slo-2* (amino acids 450–569). The second deletion mutant [*slo-2 (nf 101)*] terminates prematurely (amino acid 489), removing most of the cytoplasmic carboxyl domain. To test whether the *nf100* allele was a loss-of-function mutation, we introduced the same alterations into a *slo-2* cDNA. *Xenopus* oocytes injected with cRNA transcribed with this vector failed to produce functionally active channels (data not shown), suggesting that the deleted region is essential for channel function. Although most of the experiments were performed with the *slo-2 (nf100)* mutant, we also recorded from *slo-2 (nf101)* mutants by using the filleted worm prep. Whole-cell currents from *slo-2 (nf101)* mutant animals closely resembled those from the *slo-2 (nf100)* mutant (data not shown). Both mutants were normal with respect to locomotion, growth rate, brood size, and synaptic transmission assayed with the filleted worm preparation (data not shown).

Cell Culture. Embryonic cells were isolated and cultured as described (1) with the following modifications. Nematode eggs were not separated from adult carcasses in a sucrose gradient. Cellular debris and carcasses were removed upon filtration. Muscle cells were identified based on their distinctive morphology in cell culture. An integrated *myo-3*::GFP-transformed strain, which labeled the body wall muscle cells with GFP, verified the method of identification (1). Recordings were performed 2–4 days after plating.

Abbreviations: RNAi, RNA interference; dsRNA, double-stranded RNA.

¶To whom correspondence should be addressed. E-mail: salkoffl@pcg.wustl.edu.

RNAi Experiments. Double-stranded RNA (dsRNA) was synthesized by using standard methods described by Fire *et al.* (15) and Christensen *et al.* (1). Briefly, *Shal* (Y73B6BL.19) and *Shaker* (ZK1321.2) full-length cRNA were transcribed by using mMESSAGE *in vitro* transcription kits (Ambion, Austin, TX) in both the T3 (sense) and T7 (antisense) orientations. Template DNA was digested with DNaseI, and RNA was purified by isopropanol precipitation and resuspended in RNase-free water. dsRNA were formed by combining equimolar concentrations of sense and antisense cRNA and then heating to 65°C for 30 min followed by slowly cooling to room temperature. The size and integrity of dsRNA were assayed on Tris boric acid EDTA agarose gels. Cells were plated in L-15 control medium or L-15 medium containing 15 μg/ml dsRNA final volume. One hour after plating, the dsRNA was diluted to a final concentration of 5 μg/ml. Media containing the dsRNA were replaced each day. Electrophysiological experiments were performed 2–4 days after plating the cells.

***In Situ* Muscle Recordings.** Adult nematodes were filleted and prepared for single electrode whole-cell recording of body wall muscle as described (2, 3).

Electrophysiology. Whole-cell and single-channel recordings were obtained by using the patch-clamp technique (16). Whole-cell currents external solution contained 140 mM NaCl, 5 mM KCl, 5 mM $CaCl_2$, 5 mM $MgCl_2$, 11 mM dextrose, 5 mM Hepes, pH 7.2 with NaOH. The 200 μM Ca^{2+} and 128 mM Cl^- internal solution contained 120 mM KCl, 20 mM KOH, 4 mM $MgCl_2$, 5 mM Tris, 0.2 mM $CaCl_2$, 36 mM sucrose, and 4 mM Na_2ATP. The 128 mM Cl^- internal solution contained 120 mM KCl, 20 mM KOH, 4 mM $MgCl_2$, 5 mM Tris, 0.25 mM $CaCl_2$, 36 mM sucrose, 5 mM EGTA, and 4 mM Na_2ATP, pH 7.2 with HCl. The 10 nM Ca^{2+} and 4 mM Cl^- internal solution contained 120 mM K^+-gluconate, 20 mM KOH, 2 mM $MgCl_2$, 4 mM Mg^{2+}-$gluconate_2$, 5 mM Tris, 0.25 mM $CaCl_2$, 36 mM sucrose, 5 mM EGTA, and 4 mM Na_2ATP. The program EGTA (Ed McClesky, Oregon Health Sciences University, Vollum Institute, Portland) was used to calculate free Ca^{2+}. The solutions for single-channel recordings are indicated in the figures. Whole-cell current traces were obtained by applying voltage steps from -70 mV to $+60$ mV in 10-mV increments from a holding potential of -70 mV. Prepulse inactivation curves for SHAKER and SHAL were obtained by eliciting K^+ currents with a test potential to $+50$ mV applied after a prepulse ranging from -70 to $+25$ mV, in 5-mV steps. The normalized current during the test pulse was plotted as a function of the prepulse potential. The data were fitted with the Boltzmann equation: $I/I_{max} = \{1 + \exp[V - V_{0.5i}/k_i]\}^{-1}$, where I is the peak current, I_{max} is the peak current when the prepulse potential was -70 mV, V and $V_{0.5i}$ are the prepulse potential and half-inactivation potential, respectively, and k_i is the inactivation slope factor. The G–V curves were obtaining by converting the peak current values from the I–V relationships to conductances by using the equation: $G = I\ (V - E_K)$, where G is the conductance, I is the peak current, V is the command pulse potential, and E_K is the K^+ reversal potential. Conductance values were normalized and fitted with a Boltzmann equation: $G/G_{max} = \{1 + \exp[-(V - V_{0.5a})/k_a]\}^{-1}$, where G is the peak conductance, G_{max} is the maximal peak conductance, V and $V_{0.5a}$ are the command potential and the midpoint of activation, respectively, and k_a is the activation slope factor. Traces were amplified and filtered at 2 kHz with an Axopatch 200A (Axon Instruments, Foster City, CA) and digitized at 10 kHz. Data were analyzed by using PCLAMP 8.2 (Axon Instruments) and SIGMAPLOT 5 (Jandel, San Rafael, CA) or ORIGIN 6.0 (Microcal Software, Northampton, MA).

Results

Whole-cell patch-clamp experiments undertaken in muscle cells in culture under physiological conditions [low intracellular concentrations of chloride ion (4–10 mM) and calcium ion (10–100 nM)] revealed a voltage-dependent outward component typical of cells in many systems in that it appeared to consist of both transient and slowly inactivating currents (Fig. 1*a*). Because the *slo-2* gene was expressed prominently in muscle cells (6) we also repeated these experiments in *slo-2* mutant cells to see whether the voltage-dependent outward components differed from WT. A virtually identical outward component was seen in these *slo-2* mutant muscle cells. In Fig. 1 representative current traces are shown for both WT cells (*a*) and *slo-2* mutant cells (*b*). Currents were elicited by a series of voltage steps applied from a holding potential of -70 mV, with 10-mV voltage steps from -70 to $+60$ mV. Fig. 1 *c* and *d* shows the activation and prepulse inactivation data for a population of currents in both cell types. The overlapping data show that these currents are indistinguishable in WT and *slo-2* mutant cells with respect to voltage dependence of activation and prepulse inactivation. They were also similar but not identical with respect to amplitude [the current density was 5.9 $\pm$ 1 pA/pF (n = 11) and 11.1 $\pm$ 1.1 pA/pF (n = 7) for WT cells and *slo-2* mutants, respectively]. The somewhat larger amount of voltage-dependent current present in mutant cells could conceivably be the result of a compensatory mechanism reacting to the absence of the SLO-2 current, but this difference was not further explored. The midpoint of activation for WT was 22.4 $\pm$ 1.1 (n = 5) compared with 17.6 $\pm$ 0.4 (n = 7) for *slo-2* mutant cells. Also the midpoints of activation and inactivation obtained from those cells were not unlike those of other V-dependent K^+ channels seen in mammals and invertebrates. These properties suggested similarities to the familiar voltage-dependent K^+ currents seen in mammals and other invertebrates (17–19). The temporal course of the whole-cell currents seen in Fig. 1 *a* and *b* shows an initial rapid inactivation, followed by a slower inactivation of the plateau phase, which suggests that more than one current may be present. To explore this possibility, we fitted the prepulse inactivation data allowing the data to be fit by two Boltzmann relations (Fig. 1*e*). Both WT and *slo-2* mutant data were well fit by the sum of two Boltzmanns (Fig. 1), suggesting that two independent voltage-dependent currents were present. As will be seen below, this idea was confirmed in further experiments.

Dissection of Voltage-Dependent Currents: SHAKER (*Kv1*) and SHAL (*Kv4*). To investigate the genetic and molecular basis of the voltage-dependent component we previously created transformed strains of *C. elegans* carrying promoter-gfp reporter constructs by using the promoters of several genes encoding K^+ channels (4). These experiments included promoter-GFP reporter constructs from the *Shaker* (ZK1321.2) and *Shal* (Y73B6BL.19) genes, which are known to encode channels that carry voltage-dependent currents. The results of these experiments showed that both *Shaker* and *Shal* genes were expressed in *C. elegans* muscle (data not shown). It should be noted that there is only a single *Shaker* and *Shal* gene in *C. elegans* (5). To reveal the relative contributions of these two current components we applied the RNAi technique (15) to the cells in culture. In these experiments we worked in a *slo-2* mutant background to eliminate any potential contamination from the SLO-2 current. To remove the SHAKER component we grew the cells in culture with double-stranded *Shaker* cRNA (see *Materials and Methods*). Whole-cell patch-clamp experiments performed on these cells at 2–4 days after plating revealed that a slowly inactivating component of outward current was absent and only a fast inactivating K^+ current remained (Fig. 2*aii*). Conversely, we also removed the SHAL current by treating the *slo-2* mutant cells with full-length double-stranded *Shal* cRNA (Y73B6BL.19). In these cells only a slowly inactivating K^+ current remained that had similarities to a delayed rectifier component (Fig. 2*aiii*). These two voltage-dependent components that were removed by the RNAi technique each had distinctive features characteristic of SHAL and SHAKER currents seen in other systems such as *Drosophila* (18, 20). As seen in Fig. 2*b*, the prepulse inactivation profile for the

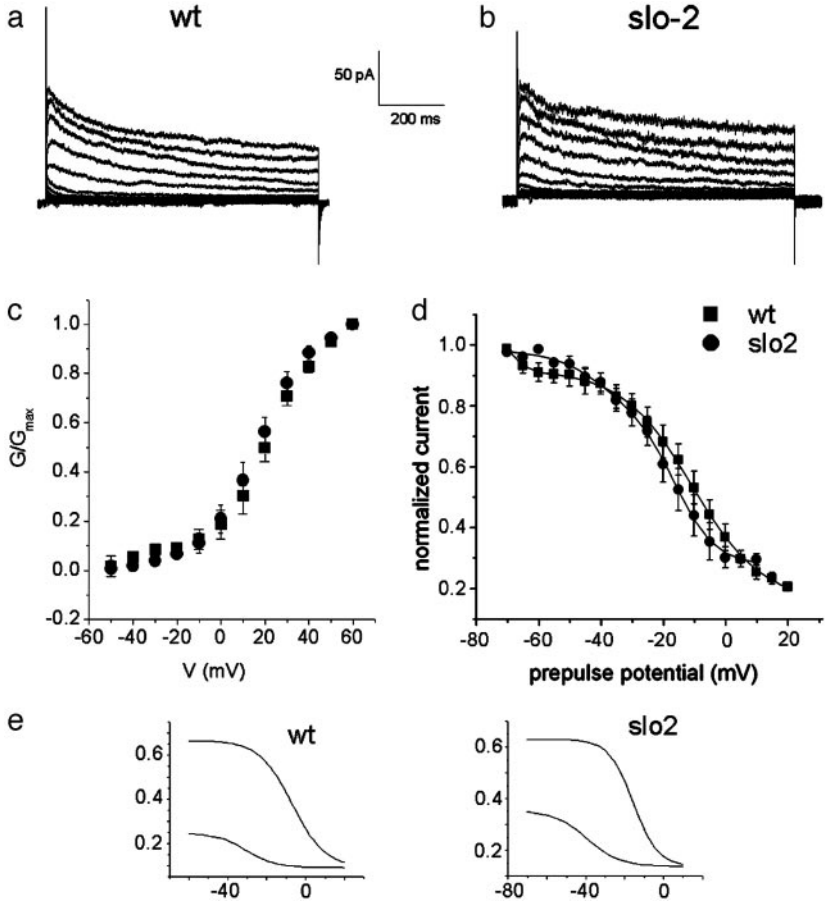

Fig. 1. The voltage-dependent outward component in WT and *slo-2* mutant cells. Comparison of whole-cell currents from a WT cell in low Ca^{2+}, low Cl^- intracellular concentrations (10 nM and 4 mM, respectively) (*a*) and a *slo-2* mutant cell (*b*). Currents were elicited from a −70 mV holding potential, in 10-mV steps from −70 to +60 mV. (*c*) *G-V* data plotted for WT cells (■; $n = 5$), in low intracellular Ca^{2+}/Cl^- solution; and *slo-2* mutant cells (●; $n = 7$). *G-V* data were plotted as described in *Materials and Methods*, using a value of −70 mV for K^+ reversal potential (E_K), which is close to the expected K^+ equilibrium potential of ≈−80 mV. (*d*) Prepulse inactivation data for WT cells (■, $n = 6$) and *slo-2* mutants (●, $n = 5$). Curves were obtained as described in *Materials and Methods* and fitted with the sum of two Boltzmann functions (1 and 2). (*e*) Each of the two components was plotted separately for both WT and slo-2 cells. The parameter values for each component were comparable between WT and *slo-2* cells, respectively: $V_{0.5(1)} = -6.9$ mV, $k_{(1)} = 8.5$; $V_{0.5(2)} = -30.9$ mV, $k_{(2)} = 7.6$ and $V_{0.5(1)} = -15.6$, $k_{(1)} = 6.33$; $V_{0.5(2)} = -39.3$ mV, $k_{(2)} = 8.4$.

SHAL component is characteristically more hyperpolarized and has a shallower slope than the SHAKER component. However, it is interesting that the nematode SHAL current described here exhibits midpoints for activation and inactivation that are relatively depolarized and significantly different from neuronal SHAL currents in mammals and invertebrates. SHAL currents inactivated with values of $V_{0.5i} = -33.1$ mV ± 1.2 and $k_i = 8.3 \pm 0.7$ ($n = 6$), whereas Shaker inactivation parameter values were $V_{0.5i} = -6.95 \pm 1.7$, $k_i = 5.8 \pm 0.5$ ($n = 2$) (note that this values are very similar for the two components that we separated in Fig. 1*e* from WT cells and *slo-2* mutant cells). The same is true for their activation curves. Whereas SHAL currents activated with values $V_{0.5a} = 11.2 \pm 1.5$ mV, $k_a = 14.1 \pm 1.04$ ($n = 5$); SHAKER currents activated at more positive potentials [$V_{0.5a} = 20.4 \pm 2$, $k_a = 7.7 \pm 1.1$ ($n = 3$)]. The removal by RNAi of both SHAKER and SHAL components in the muscle membrane resulted in leaving only a small residual leak current in the membrane as can be seen in the current remaining in Fig. 2*aii* after inactivation of the fast transient component. Thus, taken together SHAKER and SHAL K^+ channels appear to account for almost all of the voltage-dependent outward current in body wall muscle cells.

SLO-2 Is the Largest Outward Current. Because we had an indication that the SLO-2 channel was perhaps the most abundantly expressed K^+ channel in *C. elegans* it was of interest to reveal its contribution in native cells. We identified the SLO-2 component by using two independent strategies: (*i*) isolation of a null mutant of the *slo-2* gene, and comparison of currents in WT cells with currents in mutant cells; and (*ii*) comparison of currents recorded in WT cells under conditions of high vs. low concentrations of intracellular chloride ion. This latter strategy was based on an earlier study of SLO-2 heterologous expression in *Xenopus* oocytes, which revealed that these channels had an unusual requirement for cytoplasmic chloride ion (6). Both strategies produced consistent results, and the SLO-2 component was identified in muscle cells in a cell culture preparation (1) as well as in adult body wall muscle cells by using the filleted worm preparation (2, 3). We recorded whole-cell outward currents from these two preparations by using the patch-clamp technique. As expected, under physiological conditions of low intracellular chloride, only the small voltage-dependent currents were present, both in cells in culture and muscle cells *in situ* (Fig. 3 *ai* and *bi*). This result was mirrored by similar experiments in *slo-2* mutant cells in culture and muscle cells *in situ*, where only the small voltage-dependent currents were present. However, when intracellular chloride and calcium ion were raised, whole-cell recordings from WT cells in culture were dominated by a large delayed outward current that showed little or no inactivation (Fig. 3 *aiii*). This large delayed outward component was completely absent in *slo-2* mutant cells recorded under identical ionic conditions, where only the small voltage-dependent components remained (Fig. 3*aiii*). The average size of the delayed outward current from WT cells in 128 mM Cl_i^- and 200 μM Ca_i^{2+} was 86.6 ± 9 pA/pF ($n = 8$) compared with 11.1 ± 1 pA/pF ($n = 7$) from *slo-2* (*nf100*) mutant cells. These experiments suggested that SLO-2 contributed 87% of the overall delayed current in cultured muscle cells under these ionic conditions. The average size of the delayed outward current from WT cells in low Cl_i^-/Ca_i^{2+} (4 mM Cl_i^- and 10 nM Ca^{2+}) was 5.9 ± 1 pA/pF ($n = 8$), which is similar to that of mutant cells, and dwarfed by the large outward current from WT cells recorded under conditions optimal for its expression. These differences are shown in the current–voltage relationships in Fig. 3*aiv*. Because the cultured muscle cells were embryonic in origin, we confirmed our results in adult body wall muscle cells by using the filleted worm preparation (2, 3). As with cells in culture, with

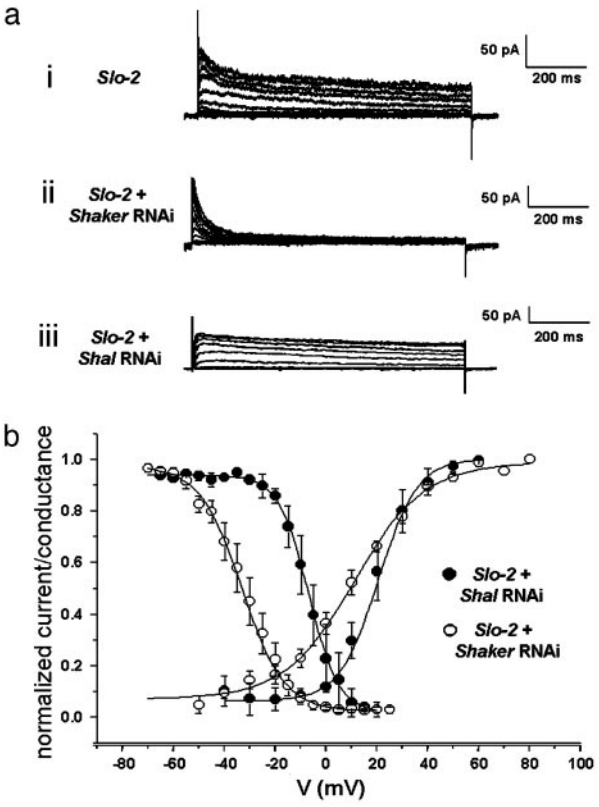

Fig. 2. Dissection of voltage-dependent components by RNAi. The *slo-2* mutant was used to obtain these data so that there would be no chance of contamination from the SLO-2 current. (*ai*) Family of K^+ currents obtained from a *slo-2* mutant muscle cell showing only the voltage-dependent components. (*aii*) Family of K^+ current traces for SHAL currents (*slo-2* mutant cell treated with *Shaker* RNAi). (*aiii*) SHAKER currents (a *slo-2* mutant cell treated with *Shal* RNAi). Cells were held at −70 mV and stepped from −70 to +60 mV in 10-mV increments. (*b*) *G-V* plots and prepulse inactivation curves for SHAL currents (○) and SHAKER currents (●). The activation parameter values were $V_{0.5a} = 11.2 \pm 1.5$ mV, $k_a = 14.1 \pm 1.04$ ($n = 5$); $V_{0.5a} = 20.4 \pm 2$, $k_a = 7.7 \pm 1.1$ ($n = 3$) for SHAL and SHAKER currents, respectively. SHAL currents inactivated with values of $V_{0.5i} = -33.1$ mV $\pm$ 1.2 and $k_i = 8.3 \pm 0.7$ ($n = 6$), whereas SHAKER inactivation parameter values were $V_{0.5i} = -6.95 \pm 1.7$, $k_i = 5.8 \pm 0.5$ ($n = 2$). Internal concentrations of Cl^- and Ca^{2+} were, respectively, 120 mM and 10 nM.

increased intracellular chloride ion, the delayed, noninactivating current was the largest component in WT cells (Fig. 3*biii*). However, in *slo-2* mutant cells, the voltage-dependent current was the larger component (Fig. 3*bii*). These results are shown in the current–voltage relationships in Fig. 3*biv*. The average delayed current measured between 800 and 900 ms at +60 mV was 130.1 ± 21 pA/pF ($n = 5$) for WT cells in 128 mM Cl_i^-, 48.8 ± 10 pA/pF ($n = 6$) for mutant cells in 128 mM Cl_i^-, and 46.6 ± 7 pA/pF ($n = 5$) for WT cells in 4 mM Cl_i^-. The maximal SLO-2 current is observed when both intracellular chloride and calcium ions are elevated. However, in the filleted worm preparation we were unable to observe the maximal contribution of the SLO-2 current because the SLO-2 current is activated by Ca^{2+} as well as Cl^-, and adult muscle cells contracted when Ca_i^{2+} was increased.

Under the conditions used in Fig. 3*aiii*, which are optimal to see the SLO-2 component of current, the relative contributions of the voltage-dependent currents can still be seen by exploiting the fact that both the SHAL and SHAKER components inactivate. Thus, the voltage-dependent components can be observed in WT cells with high intracellular $[Cl^-]$ as a subtractive inactivating component by using a prepulse inactivation protocol (Fig. 4). Using the prepulse inactivation protocol, the inactivating component appeared similar to the voltage-dependent component seen in mutant *slo-2* cells, both in amplitude and kinetic properties.

SLO-2 Single-Channel Properties in Native Cells. Single-channel openings of a high conductance K^+ channel were commonly seen in whole-cell recordings from WT but not *slo-2* mutant cells. These results suggested that these high conductance channels are encoded by the *slo-2* gene and account for the large delayed outward current in these cells. To observe single-channel properties of native SLO-2 channels and investigate their sensitivity to Ca_i^{2+} and Cl_i^-, we pulled inside-out patches from cells in culture and perfused the intracellular surface of the membrane with solutions containing different concentrations of Ca_i^{2+} and Cl_i^- (Fig. 5*a*). We observed that SLO-2 channels from cultured muscle cells required both Ca_i^{2+} and Cl_i^- for activation. In solutions lacking Ca_i^{2+} and Cl_i^- the open probability (P_o) was 0.001, which increased slightly with the addition of either Cl_i^- alone (100 mM, $P_o = 0.013$) or Ca_i^{2+} alone (100 μM, $P_o = 0.004$). However, with both Ca_i^{2+} and Cl_i^-, the P_o was dramatically increased ($P_o = 0.338$) (Fig. 5 *a* and *b*). This observation, that the P_o with both ions present is much greater than the sum of the P_os with either ion present, suggests a cooperative mechanism of sensing Ca^{2+}/Cl^- (6). The single-channel conductance of SLO-2 channels from native cells was 107.5 ± 6 pS ($n = 3$), which was similar to the single-channel conductance of the cloned SLO-2 channel expressed heterologously in *Xenopus* oocytes (6). Like cloned SLO-2 channels (6), native SLO-2 channels were slightly voltage sensitive. Voltage ramps from an inside-out patch revealed that SLO-2 channel openings were more likely with increasing depolarization (Fig. 5*c*).

The SLO-2 component is clearly the largest outward current available to the cell, but apparently its contribution to outward conductance is conditional on the intracellular ionic environment. As such, its contribution may vary from an overwhelmingly large component, to a relatively small component. Many questions regarding its role remain, such as whether it functions in normal cell physiology apart from hypoxic conditions, and whether it is a sensor for bulk internal ion concentrations or a sensor for ion concentrations in membrane-associated microdomains.

Discussion

Molecular-Genetic Resources of *C. elegans*. The molecular-genetic resources available in *C. elegans* makes this organism a particularly suitable model system to gain insight into the molecular basis of K^+ channel function and its physiological roles. Mutant analysis may also lead to revealing the *in vivo* roles of these channels with respect to behavior and coping with various environmental challenges. Previous work (7) described two types of voltage-dependent K^+ currents in adult *C. elegans* body wall muscle cells and noted that a component decreased after reducing the intracellular Cl^- concentration. However, the molecular identity of these components was not established. Here, we were able to identify the genetic components of the K^+ current in body wall muscle cells that constitute most of the outward current. This was achieved by combining two different methods that allow the selective elimination of different K^+ channel gene products: (*i*) we constructed a deletion mutant that removes the *slo-2* gene and (*ii*) we used the dsRNAi technique to individually silence the expression of the *Shaker* and *Shal* K^+ channel genes. Quite notably, this dissection of muscle membrane K^+ currents in *C. elegans* showed that only two currents, SHAKER and SHAL, contribute most of the voltage-dependent K^+ conductance in the membrane. These two currents have properties characteristic of orthologues found in many other systems (17–19). In this system the SHAKER current contributes a slowly inactivating current. In this aspect, the *C. elegans* SHAKER current more closely resembles most orthologues in mammals that have slow inactivation, in contrast to the *Drosophila* SHAKER orthologue that inactivates more rapidly (20). SHAL functions as a transient current and operates in a characteristically hyperpolarized voltage

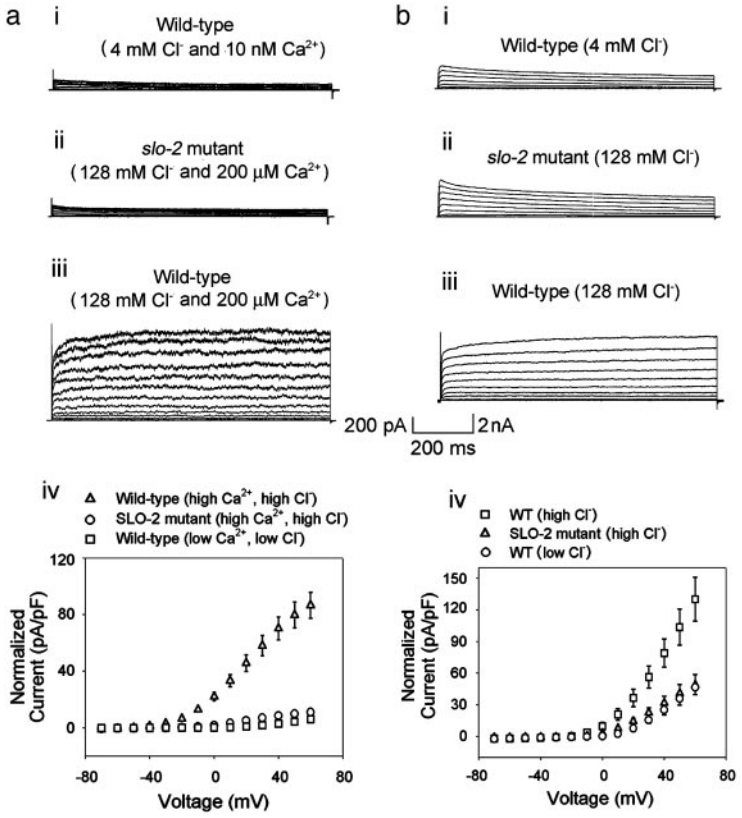

Fig. 3. SLO-2 is a major reserve component of the delayed outward current in *C. elegans*. Whole-cell currents are shown from body wall muscle cells in culture, demonstrating that SLO-2 is the major outward current in these cells. Note that the scale is changed from that in Fig. 1. so that the small amplitude of the voltage-dependent components (*ai* and *aii*) can be seen relative to the SLO-2 component (*aiii*). (*ai*) Current traces from a WT cell using low Ca^{2+} and Cl^- (10 nM and 4 mM, respectively). (*aii*) Current traces from a *slo-2 (nf100)* mutant cell using high Ca^{2+} and Cl^- internal solution (200 μM and 128 mM, respectively). (*aiii*) Current traces from a WT cell using high Ca^{2+} and Cl^- internal solution. (*aiv*) Current–voltage relationships of the currents shown in *ai–aiii*. (*b*) Whole-cell currents recorded *in situ* from body wall muscle of adult animals. (*bi*) Current–traces from a WT cell using 4 mM Cl^- internal solution. (*bii*) Current traces from a *slo-2 nf100* mutant cell using 128 mM Cl^- internal solution. (*biii*) Current traces from a WT cell using 128 mM Cl^- internal solution. Free internal Ca^{2+} was 10 nM in these experiments. (*biv*) Comparison of current–voltage relationships of currents shown in *bi–biii*.

range with respect to both its activation and inactivation. These currents function in an intracellular environment, which, if typical of most systems, has a rather low (≈10 mM) concentration of intracellular chloride ions (9). In contrast, SLO-2 channels have an absolute requirement for Cl^- (6) and are largely inactive under those conditions.

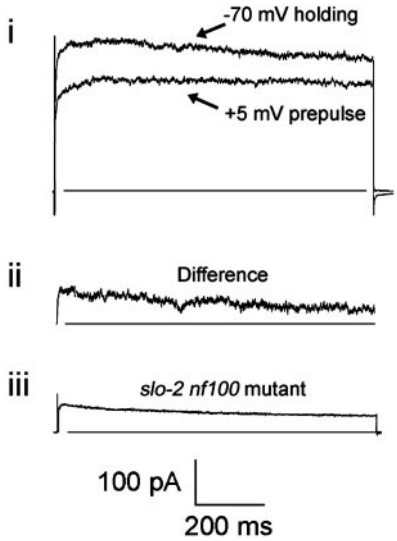

Fig. 4. Separation of the voltage-dependent inactivating currents from the SLO-2 current in a WT cell. (*ai*) Current traces of test pulses at +50 mV. Top trace is before, and bottom trace is after a 1-s conditioning prepulse at +5 mV; the holding potential was −70 mV. (*aii*) The difference between the two currents in *ai* shows the inactivating component alone. (*aiii*) Current trace of a *slo-2 nf100* mutant muscle cell in culture at +50 mV (−70 mV holding potential). For comparison, the current amplitude was scaled to the same amplitude as the trace shown in *aii*.

Size of the SLO-2 Component. One puzzling question has to do with the extraordinarily large size of the SLO-2 current relative to the voltage-dependent currents when high Cl^- is present. If the SLO-2 current were completely functional in a muscle cell almost certainly the muscle would be unable to contract. However, one indication that the SLO-2 current is a reserve current (i.e., held in reserve and not usually active) is the fact that *slo-2* loss-of-function mutants have no obvious phenotype except that they are more susceptible to death under hypoxic conditions (8). The fact that these mutant worms do not show any obvious defect in locomotion suggests that the SLO-2 channels are not very active in muscle under normal physiological conditions. This also implies that intracellular Cl^- and Ca^{2+} concentrations are normally fairly low as in other metazoan systems. However, because intracellular calcium is expected to rise during muscle contraction, it is not out of the question that the SLO-2 current is activated to a small degree under normal physiological conditions. In addition to the *slo-2* gene, the *slo-1* gene, which encodes high-conductance calcium-activated K^+ channels, is also expressed in *C. elegans* body-wall muscle, as evidenced by promoter-GFP expression experiments (3). However, its total contribution to total outward current in these cells must be very small. A comparison of outward currents from WT and *slo-1* mutant cells did not, as in the *slo-2* study, show any obvious differences (data not shown). Indeed, as we have shown in Figs. 1–3, the currents remaining in *slo-2* mutant cells consist primarily of small voltage-dependent components, and even in the presence of high internal calcium ion there is no evidence of another significant component.

Relation to the Vertebrate Na^+-Activated K^+ Channel. The SLO-2 channel is the *C. elegans* orthologue of the Na^+-activated K^+ channel (8), prominent in vertebrate heart and brain (21), and

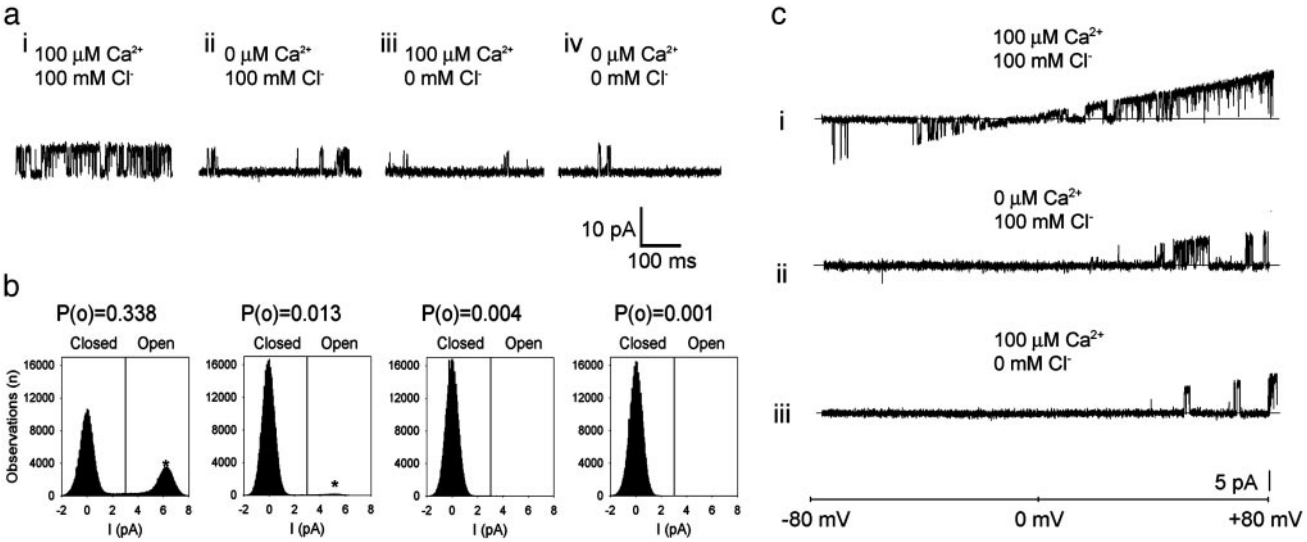

Fig. 5. (*a*) Single-channel SLO-2 currents from an inside-out patch from a WT muscle cell in culture. The intracellular surface of the membrane was perfused with Ca_i^{2+} and Cl_i^- concentrations as indicated while the (intracellular) membrane potential was held at +40 mv. Perfusion with 100 μM Ca_i^{2+} and 100 mM Cl_i^- produced periods of high activity followed by periods of inactivity. Records shown are from periods of higher activity in each condition. (*b*) Analysis of open probability and plots of an all-points histogram for 20-s intervals. Each plot is shown directly below the current traces for each condition. A 20-s interval was chosen for analysis of each condition because it was much longer than the longest inactive state. An asterisk indicates the peak of the single-channel level in the all-points histograms. Similar channels were not seen in patches from *slo-2 nf100* mutant cells ($n = 7$). (*c*) Voltage ramps (−80 to +80 mV) of an inside-out patch perfused with Ca_i^{2+} and Cl_i^- concentrations as indicated. The duration of the ramp was 1,600 ms. The pipette (external) solution contained 120 mM K^+-gluconate, 20 mM KOH, 2 mM $MgCl_2$, 4 mM Mg^{2+}-$gluconate_2$, 5 mM Tris, 0.25 mM $CaCl_2$, 36 mM sucrose, 5 mM EGTA, and 4 mM Na_2ATP. The bath (internal) solutions contained 100 mM KCl or 100 mM K^+-gluconate, 59 mM K^+-gluconate, 10 mM Hepes, 1 mM KOH, and 0.1 mM Ca^{2+}-$gluconate_2$, pH 7.2, with KOH. The Ca^{2+}-free solutions contained 100 mM KCl or 100 mM K^+-gluconate, 30 mM K^+-gluconate, 10 mM Hepes, 30 mM KOH, and 11 mM EGTA, pH 7.2, with KOH.

hypothesized to serve as a protective mechanism against ischemia and hypoxia (21, 22). Because mutants of *slo-2* in *C. elegans* are hypersensitive to hypoxia (8) it is likely that protection against hypoxia is a conserved role for SLO-2 channels. The activity of mammalian SLO-2 channels is also enhanced by intracellular chloride (8). Perhaps of direct relevance is the fact that intracellular chloride is reported to rise to ≈55 mM in instances of simulated hypoxia (9). Conceivably, a large number of SLO-2 channels may serve as a mechanism for the earliest possible interception and reversal of the pathological conditions that accompany hypoxia, namely a pathological rise in the bulk concentrations of intracellular ions.

Reserve Membrane Conductances. Another possible reason for an excessively large number of channels present in a cell has to do with a biophysical design whereby only a tiny percentage of channels are active at any one time. This design termed the "spare channel" hypothesis (23) has been postulated for ATP-sensitive channels and involves maintaining the membrane potential stable and unreactive to minor fluctuations in conductance. Whether such a mechanism could be at work with regards to SLO-2 channels remains to be determined. The results presented here account for the major outward conductance present in the membrane, which is seen under typical physiological conditions, and a major reserve conductance, which is likely to be activated during conditions of hypoxia. A second reserve conductance likely to be activated is the *twk-18* component, which is responsive to elevated temperature and pH (10). However, because of the very low open channel probability of this channel, it is not likely to be a large component of outward conductance under most circumstances. Other TWK channels present in the membrane could be conditional on other factors yet to be determined or could account for the resting conductance of the membrane. Taken together these results could reflect a general picture of complex membrane electrical properties common to many cells but not often detected. Conceivably, many cells could have a small number of household conductances that function under normal circumstances, but additional "hidden" conductances that are activated only during unusual circumstances.

This work was supported by National Institutes of Health Grants R24 RR017342-01 and R01 GM067154-01A1 (to L.S.) and a grant from the Washington University McDonnell Center for Cellular and Molecular Neurobiology. P.R. is supported by a Consejo Nacional de Investigaciones Científicas y Técnicas doctoral fellowship, Fondo Nacional de Investigacion Científica y Tecnologica Grant 2010006, Centro de Estudios Científicos, and Fundacion Andes. Centro de Estudios Científicos is a Millennium Institute.

1. Christensen, M., Estevez, A., Yin, X., Fox, R., Morrison, R., McDonnell, M., Gleason, C., Miller, D. M., 3rd & Strange, K. (2002) *Neuron* **33,** 503–514.
2. Richmond, J. E. & Jorgensen, E. M. (1999) *Nat. Neurosci.* **2,** 791–797.
3. Wang, Z. W., Saifee, O., Nonet, M. L. & Salkoff, L. (2001) *Neuron* **32,** 867–881.
4. Salkoff, L., Butler, A., Fawcett, G., Kunkel, M., McArdle, C., Paz-y-Mino, G., Nonet, M., Walton, N., Wang, Z. W., Yuan, A. & Wei, A. (2001) *Neuroscience* **103,** 853–859.
5. Bargmann, C. I. (1998) *Science* **282,** 2028–2033.
6. Yuan, A., Dourado, M., Butler, A., Walton, N., Wei, A. & Salkoff, L. (2000) *Nat. Neurosci.* **3,** 771–779.
7. Jospin, M., Mariol, M.-C., Ségalat, L. & Allard, B. (2002) *J. Physiol. (London)* **544,** 373–384.
8. Yuan, A., Santi, C. M., Wei, A., Wang, Z-W., Pollak, K., Nonet, M., Kaczmarek, L., Crowder, C. M. & Salkoff, L. (2003) *Neuron* **37,** 765–773.
9. Lai, Z. F. & Nishi, K. (1998) *Am. J. Physiol.* **275,** H1613–H1619.
10. Kunkel, M. T., Johnstone, D. B., Thomas, J. H. & Salkoff, L. (2000) *J. Neurosci.* **20,** 7517–7524.
11. O'Connell, A. D., Morton, M. J. & Hunter, M. (2002) *Biochim. Biophys. Acta* **1566,** 152–161.
12. Jansen, G., Hazendonk, E., Thijssen, K. L. & Plasterk, R. H. (1997) *Nat. Genet.* **17,** 119–121.
13. Liu, L. X., Spoerke, J. M., Mulligan, E. L., Chen, J., Reardon, B., Westlund, B., Sun, L., Abel, K., Armstrong, B., Hardiman, G., *et al.* (1999) *Genome Res.* **9,** 859–867.
14. Wei, A., Yuan, A., Fawcett, G., Butler, A., Davis, T., Xu. S. Y. & Salkoff, L. (2002) *Nucleic Acids Res.* **30,** E110–R0.
15. Fire, A., Xu, S., Montgomery, M. K., Kostas, S. A., Driver, S. E. & Mello, C. C. (1998) *Nature* **391,** 744–745.
16. Hamill, O. P., Marty, A., Neher, E., Sakmann, B. & Sigworth, F. J. (1981) *Pflügers Arch.* **391,** 85–100.
17. Connor, J. A. & Stevens, C. F. (1971) *J. Physiol. (London)* **213,** 21–30.
18. Wei, A., Covarrubias, M., Butler, A., Baker, K., Pak, M. & Salkoff, L. (1990) *Science* **248,** 599–603.
19. Nadal, M. S., Ozaita, A., Amarillo, Y., Vega-Saenz de Miera, E., Ma, Y., Mo, W., Goldberg, E. M., Misumi, Y., Ikehara, Y., Neubert, T. A. & Rudy, B. (2003) *Neuron* **37,** 449–461.
20. Salkoff, L. & Wyman, R. (1981) *Nature* **293,** 228–230.
21. Dryer, S. E. (1994) *Trends Neurosci.* **17,** 155–160.
22. Kameyama, M., Kakei, M., Sato, R., Shibasaki, T., Matsuda, H. & Irisawa, H. (1984) *Nature* **309,** 354–356.
23. Cook, D. L., Satin, L. S., Ashford, M. L. J. & Hales, C. N. (1988) *Diabetes* **37,** 495–498.